The Astrophysical Journal Letters, 741:L15 (4pp), 2011 November 1 doi:10.1088/2041-8205/741/1/L15

MEASUREMENT OF THE ELECTRIC CURRENT IN A kpc-SCALE JET

P. P. Kronberg[1,2], R. V. E. Lovelace[3], G. Lapenta[4], and S. A. Colgate[5]
[1] Theoretical Division T-2, Los Alamos National Laboratory M.S. B283, Los Alamos, NM 87545, USA; kronberg@lanl.gov
[2] Department of Physics, University of Toronto, Toronto, ON M5S 1A7, Canada
[3] Department of Astronomy, Cornell University, Ithaca, NY 14853-6801, USA; lovelace@astro.cornell.edu
[4] Centre for Plasma Astrophysics, Departement Wiskunde, Katholieke Universiteit Leuven, Belgium; giovanni.lapenta@kuleuven.be
[5] Los Alamos National Laboratory, Los Alamos, NM 87545, USA; colgate@lanl.gov
Received 2011 May 4; accepted 2011 September 26; published 2011 October 12

ABSTRACT

We present radio emission, polarization, and Faraday rotation maps of the radio jet of the galaxy 3C303. From these data we derive the magnetoplasma and electrodynamic parameters of this 50 kpc long jet. For one component of this jet we obtain for the first time a direct determination of a *galactic*-scale electric current ($\sim 3 \times 10^{18}$ A), and its direction—*positive* away from the active galactic nucleus. Our analysis strongly supports a model where the jet energy flow is mainly electromagnetic.

Key words: galaxies: jets – galaxies: magnetic fields – plasmas

1. INTRODUCTION

A fundamental conundrum of astrophysical jet models is how energy is extracted from the accretion flow close to the black hole event horizon. The total energy carried by the jets of active galaxies is estimated to be a non-negligible fraction of the supermassive black hole formation energy, $\sim 0.1 M_{\rm bh}c^2$ (Kronberg et al. 2001). The jets are initially highly relativistic and low density, and for this reason are thought to be *magnetically dominated* or force-free with a negligible fraction of the power in particle kinetic energy. That is, the energy outflow from the accretion disk is in the form of a collimated "Poynting-flux jet" as proposed by Lovelace (1976) and Blandford (1976), and subsequently studied in many papers (Benford 1978; Lovelace et al. 1987, 2002; Lynden-Bell 1996; Li et al. 2001; Lovelace & Romanova 2003; Nakamura et al. 2008). The model has a current outflow (or inflow) I_z along the spine of the jet of cylindrical radius r_J initially of the order of the Schwarzschild radius of the black hole. The associated toroidal magnetic field is responsible for collimating the jet. An equal but opposite "return current" flows inward (or outward) at much larger distances from the jet axis so that the net current outflow from the source is zero. Because the jet current and its return have opposite signs, they repel as a result of their magnetic interaction mediated by the toroidal magnetic field B_ϕ. This repulsion between the jet and its (more spatially distributed) return current has been demonstrated in MHD simulations (Ustyugova et al. 2000, 2006; Nakamura et al. 2008).

Rotation measure (RM) gradients observed on parsec scales close to the nuclear central black hole have provided evidence consistent with an electric current flow (Asada et al. 2002; Gabuzda et al. 2004; Zavala & Taylor 2005). Here, on a scale 10^4 times larger in a "mature" jet, we present a measured estimate of the jet's net axial current and its sign.

2. BRIEF DESCRIPTION OF THE OBSERVATIONS

3C303 was observed in the Very Large Array's (VLA) most extended "A" configuration in Stokes parameters I, Q, U in the 1.4, 4.9, and 15 GHz radio bands with maximal $u - v$ coverage over an 11.5 hr observing period in 1981 April. Calibrated images have been discussed and analyzed in Kronberg (1986) and Lapenta & Kronberg (2005, hereafter LK05). In 2010 and 2011, the 1.4 and 4.9 GHz images were re-edited (flagged), re-calibrated, and re-imaged using more updated AIPS imaging procedures, partly as a check of the earlier 1980s imaging procedures. We found excellent correspondence, though the more recent procedures permitted better imaging of the faintest structures. Due to the higher noise levels and sparser aperture plane ($u - v$) coverage of the 15 GHz data they are not presented here, though they are useful for confirming the main image features at a resolution of $\sim 0\farcs15$ and the lack of any detectable Faraday rotation between 15 and 4.9 GHz.

3. THE JET STRUCTURE AND KNOTS OF 3C303

The 3C303 radio source at $z = 0.141$ (Figures 1 and 2) has a one-sided prominent jet with regular repeating knot structures in both VLA radio (Kronberg 1976, 1986; Lapenta & Kronberg 2005 (LK05) and *Chandra* X-ray bands (Kataoka et al. 2003). It resides in a relatively sparsely populated intergalactic environment and at a high galactic latitude [$(l, b) = +90\fdg5, +57\fdg5$]. Being away from a galaxy cluster, it is well suited to an analysis of Faraday RM within the jet and lobes, since competing Faraday RM from an immediate cluster environment and the Galactic foreground are small. Given this situation, we applied improved, new determinations of the RMs of neighboring background radio sources (Kronberg & Newton-McGee 2011). This allows the most accurate available estimate of the "RM zero level," so that our observed RM gradients and RM = 0 crossings are minimally affected by foreground plasma (Section 5).

The above combination of radio and X-ray images plus background source's RMs permits the jet's physical parameters, including its current, to be analyzed in isolation. 3C303's radiating knots are large, a few *thousand* times larger in volume than those in, for example, the well-studied nearby M87 radio galaxy. The laterally unresolved "spine" of its jet is surrounded by a "cocoon" of relativistic, radio- and X-ray-visible, gas mixed with thermal plasma which has both a low plasma β (ratio of plasma pressure to magnetic pressure) and a highly ordered magnetic field structure (Figure 1).

The plasma β, along with the other plasma parameter, and minimum energy estimates are derived and presented in LK05, which can be consulted for further details. We distinguish the jet spine, of cylindrical radius r_J normal to the propagation direction (z) and which is laterally unresolved and appears

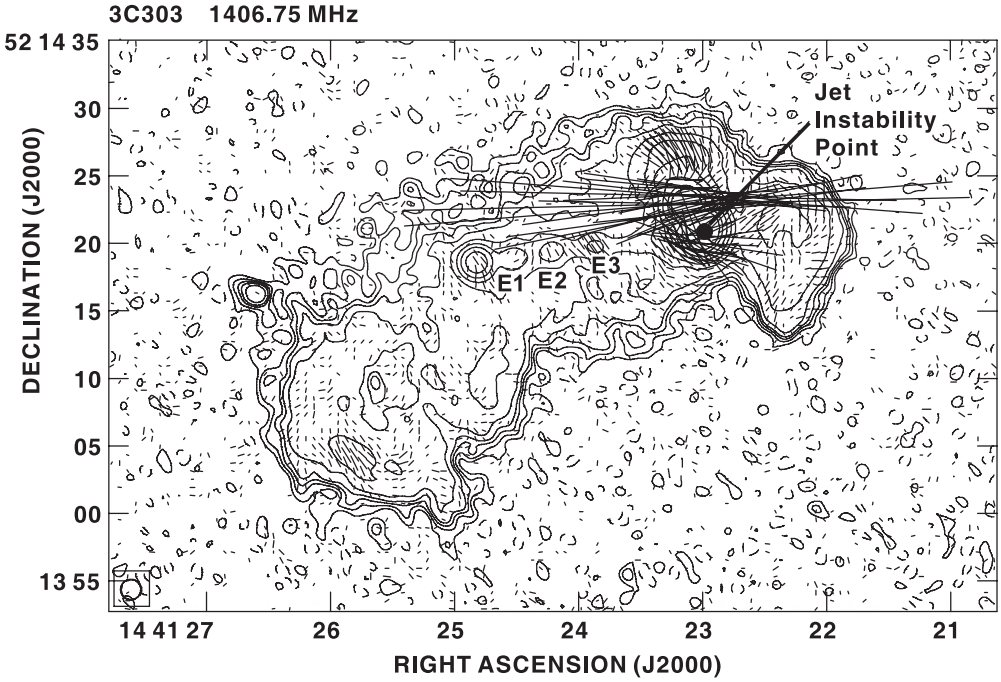

Figure 1. 1.4 GHz, 1.″5 resolution VLA image of the entire 3C303 system showing an apparent counterjet knot, the highly polarized western lobe, and a continuation of the jet to its final western stopping point. Linear polarization lines are scaled such that a 1″ equivalent length = 2.5 mJy beam^{-1}. *I* contours are shown at −0.5, 0.5, 1, 1.5, 2, 3, 6, 12, 24, 50, 100, and 150 mJy beam^{-1}.

to carry the jet power, from the "knots," which are partially resolved "cocoons" around the unresolved "spine." The cocoons contain a mix of magnetized thermal and relativistic plasma. We find no detectable growth in the knot widths away from the active galactic nucleus (AGN), which puts an *upper limit* of 0.°7 on the opening angle of the jet.

The jet's regular structure, combined with the appearance of a transverse, magnetically coherent, western lobe complex also suggests it has a clear laboratory of jet disruption. The disruption point is indicated in Figure 1. Model simulations by LK05 applied MHD soliton-like solutions of the Grad–Shafranov equation to the radio and X-ray radio images of the regular knot structure of the 3C303 jet. Their models successfully computed jet stability times and constrained its plasma parameters. The above analysis forms a basis for this Letter, independent of the MHD model details in LK05. It is the visible, synchrotron radiating cocoon surrounding the jet that enables us to probe the current, most of which is probably confined to the unresolved "spine." It is also apparent that the jet continues beyond the disruption point in Figure 1 and terminates in a bow-shock-like extremity to the west. To the east, a large polarized loop is also seen, as well as a possibly related "counter hot spot" that aligns with the western jet. We do not attempt interpretation of these latter two features in this Letter and defer them to a following paper.

Below, we describe a rare opportunity to measure the Faraday rotation (RM) variation transverse to, and along, a segment of the jet in knot E3 (Figure 1). Combined with the full plasma diagnostics and a determination of the RM zero level from surrounding sources, this provides, for the first time, a direct estimate of both the magnitude and sign of a jet's *electric current* on kiloparsec (kpc) scales in a low-density intergalactic environment.

The partial resolution of the knots in the VLA images at 1.4 and 4.9 GHz permits estimates of the relativistic gas density

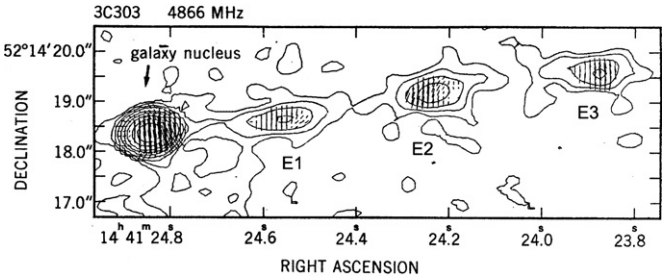

Figure 2. 4.9 GHz VLA image of the 3C303 jet at 0.″35 resolution showing the three prominent, elongated, and equally spaced knots E1, E2, and E3 to the right of the stronger, variable milliarcsec-size galaxy nucleus source.

and approximate magnetic field energy within each kpc-scale synchrotron radiating knot (cocoon).

The first stage in measuring the jet current is to calculate the approximate magnetic field strengths in the knots using the analysis described in LK05. Note that the knots' equipartition magnetic field strength estimates depend only weakly on the volume filling ϕ, as $\phi^{-2/7}$, and on the upper cutoff frequency of the photon spectrum of the jet's emission. The latter extends to 10^{17} Hz (Kataoka et al. 2003), and its reduction by, say 100×, would reduce the (redshift-corrected) total energy content in the knots by only 30%. At lower particle energies, the uncertain extrapolation of the knots' relativistic particle energy spectrum, corresponding to (unobserved) very low radio frequencies, could in principle raise our estimate of $|B|$ by a modest factor less than unity; however, no anomalously steep spectrum between 1.4 and 4.9 GHz is seen in the region of the 3C303 jet.

We estimate a field strength in 3C303's jet knots, where $B_{\rm knot} \sim 0.5$ mG (LK05), measured with a 0.″35 beam and allowing for some out-of-plane component due to the expected helical form of the jet's magnetic field.

At the 0.″35 resolution of the 4.9 GHz VLA image (Figure 2), the projected line-of-sight magnetic field orientation within

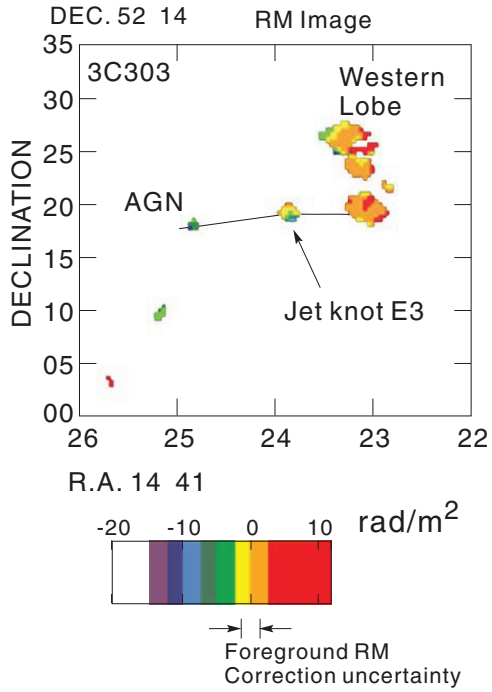

Figure 3. Faraday rotation image of the 3C303 radio source at a resolution of 1.″5. The RM zero level has been corrected by 18 ± 4 rad m^{-2} (see the text).

each knot is parallel to the jet axis. The 4.9 GHz percentage polarizations of knots E_1, E_2, and E_3 are ∼27%, 21%, and 26%, respectively, and the knots are elongated in the projected jet direction by ∼2.″2.

4. THE FARADAY ROTATION AND THERMAL ELECTRON DENSITY

Figure 3 shows the two-dimensional RM variation within the brighter parts of the entire 3C303 system derived from the 1.4 and 4.9 GHz images at a common 1.″5 resolution. Values range between +5 and +25 rad m^{-2} over a maximum extent of ∼50″, including 3C303's extended western lobe. No higher RMs are seen anywhere within the source boundaries. One test for a 180° ambiguity in $\chi(\lambda^2)$ is to separately produce Q and U images at the higher frequency of 5 GHz, where we can test for "exchanges" between Q and U along the jet. None were found, meaning that no substantially higher RMs occurred in or around the jet. This is consistent with the spatially smooth and continuous behavior of the observed RM distribution, and the modest overall range of observed RMs. The absence of any very high RMs is further confirmed from our 15 GHz observations (Section 2), which are close in λ^2 to the 4.9 GHz polarization angles. All of these "tests" confirm beyond reasonable doubt that our RM image from just two wavelengths accurately reflects the true RM distribution. 3C303's integrated RM, determined from polarization data at six frequencies, is $+18 \pm 2$ rad m^{-2} (Simard-Normandin et al. 1981). This is nicely concordant with the RM range in Figure 3, after the −18 rad m^{-2} correction above for the independent foreground RM estimate in Section 5 below.

The jet knot E3 is resolved just enough, both across and along the jet, to show an RM gradient that is transverse to the jet axis—whose orientation (solid line in Figure 3) was determined independently from the local jet ridge line defined by the total radiation (I). The varying RM in knot E3 also confirms the presence of some thermal plasma in the cocoon. The RM gradient, ∇RM, and its sign in a $y - z$ patch of sky around knot E3, is ∼+10 rad m^{-2} kpc^{-1}. Within the conservatively clipped knot E3 boundary in Figure 3 the RM is resolved in two dimensions over $\mathcal{O}(8)$ independent sampling points (defined as 2 per FWHM beamwidth in each dimension). If we were to expand the boundary by 15%, where there is still RM signal, it would include $\mathcal{O}(11)$ sampling points. Even for the tighter cocoon boundary in Figure 3 there is sufficient signal and resolution to define the direction and magnitude of the vector, ∇RM within the knot E3 cocoon.

Having measured a differential RM over the knot, its dimension, and the approximate magnetic field strength, we can estimate the non-relativistic plasma density within the knot via the following equation:

$$\mathrm{RM} = 4.1 \times 10^5 \left(\frac{n_e}{\mathrm{cm}^{-3}}\right)\left(\frac{B_\parallel}{\mathrm{mG}}\right)\left(\frac{x}{500\,\mathrm{pc}}\right)\frac{\mathrm{rad}}{\mathrm{m}^2} \approx 10\frac{\mathrm{rad}}{\mathrm{m}^2}, \quad (1)$$

where x is the line-of-sight distance through the knot. Inserting $B_\parallel$ and x gives $n_e \sim 1.4 \times 10^{-5}$ cm^{-3}, similar to the value obtained in LK05.

An independent estimate of n_e can be made from the observed polarization *degree* in the knots. On the reasonable assumption that the very regular field geometry in knot $E3$ results from a helical geometry, knot-internal Faraday dispersion is limited by the high observed degree of polarization ≃25% at 5 GHz. This test implies a back-to-front, knot-internal differential Faraday rotation at 5 GHz of $\lesssim 30°$, consistent with the knot's RM observed above (LK05). It is consistent with the above n_e estimate and gives us confidence in the local n_e scaling that is required to estimate the jet current—which we discuss next.

This low value of n_e outside the jet spine points to a magnetically confined (or dominated) jet (LK05): confinement of the jet by hot gas at X-ray temperatures is not possible because $p_{\mathrm{gas}} = n_e k T_X \ll \mathbf{B}^2/8\pi$. A common feature of the magnetic jets is that the internal pressure of the magnetic field $B^2_{\mathrm{knot}}/8\pi$ (and relativistic particles) is confined by the pinch force of the external toroidal magnetic field $B_\parallel$. The models give $B_{\mathrm{knot}} \sim B_\parallel$ (LK05).

5. ESTIMATE OF THE ELECTRIC CURRENT IN THE 3C303 JET

An important final step in relating (∇RM) to an axial current is to calibrate the RM zero level. We averaged discrete source RMs along neighboring lines of sight to 3C303 from a recent accurate RM data set (Simard-Normandin et al. 1981; Kronberg & Newton-McGee 2011). The resulting RM zero-level correction, -18 ± 4 rad m^{-2}, has been applied to the RM scale of Figure 3. With this zero-level correction, we find that the RM in knot E3 changes sign *on* the jet axis, within the limit of our uncertainties. Furthermore, its gradient ($\nabla\mathrm{RM} = n_e B_\phi$) is found to be perpendicular to the (independently measured) axis of knot E3 and the jet axis. This corresponds to the expected RM behavior around an electric current flowing along a jet's axis.

The reversal of the RM sign on the jet axis matches the signature of a current-carrying cylinder, where we are measuring the azimuthal component of a helical magnetic field at distances $\approx y$ on opposite sides of the synchrotron radiating cocoon surrounding the unresolved spine of the jet. The inferred current, $I_z \propto (y/n_e)\nabla\mathrm{RM}$, is the total current within the cocoon's radius

y, over which we have measured the transverse ∇RM. Thus, within knot E3

$$I_z \sim 7.7 \times 10^{18} \left(\frac{B_\phi}{\mathrm{mG}}\right)\left(\frac{y}{0.5\,\mathrm{kpc}}\right)\mathrm{A}, \quad (2)$$

where B_ϕ is the toroidal component of magnetic field at a distance y in the sky plane from the jet (z) axis. The positive sign of the gradient ∇(RM) indicates that a current of $\sim 3.85 \times 10^{18}$ A, for $B_{\mathrm{equi}} = 0.5$ mG, is directed *away* from the galaxy nucleus. That is, within 0.5 kpc of the jet axis there is a net flow of negative charge toward the AGN core within knot E3.

Our result for the jet current is subject to different corrections and adjustments: for example, (1) if the jet axis is significantly out of the plane of the sky then the observed RM gradient can arise from a purely toroidal field, but a helical field would in this case shift the RM = 0 line away from the jet's axis, contrary to the present observations. (2) In another example, if the magnetic field of the jet is not symmetric about its axis the field estimates will be modified. Such possibilities, especially (1), underline the importance of establishing from observations, an optimally foreground-free RM (y, z) over the source image, as we have done here. Considering these uncertainties and the limited angular resolution, our best estimate of the axial jet current at knot E3 is $10^{18.5\pm0.5}$ A. This is the first direct estimate of a current in a kpc-scale extragalactic jet.

6. DISCUSSION AND IMPLICATIONS

A magnetically dominated jet can be modeled as a transmission line running in the z-direction with the electric potential drop across it ΔV. This is equal to the potential drop across the black hole accretion disk from its inner-to-outer radius (Lovelace 1976; Lovelace & Ruchti 1983). A typical value is $\Delta V \sim 10^{20}\, V(B_{\mathrm{bh}}/10^4\,\mathrm{G})(M_{\mathrm{bh}}/10^8\,M_\odot)$, where B_{bh} is the poloidal magnetic field strength near the black hole and M_{bh} is its mass (Lovelace 1976). The current flow in this "transmission line" is $I_z = \Delta V/Z$, where the impedance of a *relativistic* jet is $Z \sim c^{-1}(\mathrm{cgs}) = (4\pi)^{-1}(\mu_0/\epsilon_0)^{1/2}(\mathrm{MKS}) = 30\Omega$ (Lovelace 1976). More generally, for a jet with bulk axial velocity u_z, $Z = (1/c)(u_z/c)$ (Lovelace & Romanova 2003). The electromagnetic power transported by the jet is $L_{\mathrm{jet}} = I_z^2 Z$.

We can now apply these ideas to the 3C303 system. The total photon luminosity L_{rad} integrated from 10^8 Hz to 10^{17} Hz is about 3.7×10^{41} erg s^{-1} or 3.7×10^{34} W (LK05). The radiated power is expected to be significantly less than the jet power because the jet power goes into a combination of pdV work on the ambient medium, and to energizing electrons and ions around the jet and in the outer radiating lobes. Thus, we let $L_{\mathrm{rad}} = \varepsilon L_{\mathrm{jet}}$, where $\varepsilon < 1$ is an efficiency factor. Substituting the observed values of L_{rad} and I_z we find

$$\varepsilon = \frac{L_{\mathrm{rad}}}{I_z^2 Z} \approx 10^{-3}\left(\frac{L_{\mathrm{rad}}}{3.7 \times 10^{34}\,\mathrm{W}}\right) \times \left(\frac{3.85 \times 10^{18}\,\mathrm{A}}{I_z}\right)^2 \left(\frac{0.1c}{u_z}\right), \quad (3)$$

where we have normalized the jet bulk velocity to $0.1c$. Note that ε is safely less than unity, and the model of Poynting flux transport of jet energy in 3C 303's black hole/accretion disk system appears to be self-consistent.

The system evidently needs to incorporate a "transducer" that converts the Poynting energy flux into high energy particles which then produce synchrotron radiation. These issues and the complex lobe structure will be discussed in a subsequent paper.

We thank Rick Perley, Robert Reid, Justin Linford, and Greg Taylor for help and advice with the re-calibrated images, Hui Li for discussion of current flow in jets, and an anonymous referee for a valuable correction to our estimate of the jet current. Support is acknowledged from a Natural Sciences and Engineering Research of Canada Discovery Grant (P.P.K.) and from NSF and NASA (R.V.E.L.).

REFERENCES

Asada, K., Inoue, M., Uchida, Y., et al. 2002, PASJ, 54, L39
Benford, G. 1978, MNRAS, 183, 29
Blandford, R. D. 1976, MNRAS, 176, 465
Colgate, S. A., & Furth, H. P. 1960, Phys. Fluids, 3, 982
Gabuzda, D. C., Murray, E., & Cronin, P. 2004, MNRAS, 351, L89
Kataoka, J., Edwards, P., Georganopoulos, M., Takahara, F., & Wagner, S. 2003, A&A, 399, 91
Kronberg, P. P. 1976, ApJ, 203, L47
Kronberg, P. P. 1986, Can. J. Phys., 64, 449
Kronberg, P. P., Dufton, Q. W., Li, H., & Colgate, S. A. 2001, ApJ, 560, 178
Kronberg, P. P., & Newton-McGee, K. J. 2011, PASA, 28, 171
Lapenta, G., & Kronberg, P. P. 2005, ApJ, 625, 37 (LK05)
Li, H., Lovelace, R. V. E., Finn, J. M., & Colgate, S. A. 2001, ApJ, 561, 915
Lovelace, R. V. E. 1976, Nature, 262, 649
Lovelace, R. V. E., Li, H., Koldoba, A. V., Ustyugova, G. V., & Romanova, M. M. 2002, ApJ, 572, 445
Lovelace, R. V. E., & Romanova, M. M. 2003, ApJ, 596, L159
Lovelace, R. V. E., Wang, J. C. L., & Sulkanen, M. E. 1987, ApJ, 315, 504
Lynden-Bell, D. 1996, MNRAS, 279, 389
Nakamura, M., Tregillis, I. L., Li, H., & Li, S. 2008, ApJ, 686, 843
Simard-Normandin, M., Kronberg, P. P., & Button, S. 1981, ApJ, 45, 97
Ustyugova, G. V., Koldoba, A. V., Romanova, M. M., & Lovelace, R. V. E. 2006, ApJ, 646, 304
Ustyugova, G. V., Lovelace, R. V. E., Romanova, M. M., Li, H., & Colgate, S. A. 2000, ApJ, 541, L21
Zavala, R. T., & Taylor, G. B. 2005, ApJ, 626, L73